EXPERIMENTAL IN-PLANE CYCLIC RESPONSE OF MASONRY WALLS WITH CLAY UNITS

Guido Magenes[1] Paolo Morandi[2] and Andrea Penna[3]

[1]*Associate professor, Dept. of Structural Mechanics, University of Pavia and EUCENTRE, Pavia, Italy*
[2]*Post-Doc Research Fellow, Dept. of Structural Mechanics, University of Pavia and EUCENTRE, Pavia, Italy*
[3]*Researcher, European Centre for Training and Research in Earthquake Engineering EUCENTRE, Pavia, Italy*
Email: guido.magenes@unipv.it, paolo.morandi@unipv.it, andrea.penna@eucentre.it

ABSTRACT :

A coordinated research, sponsored under the European ESECMaSE project, gave the occasion to gain additional useful information on the cyclic behaviour of masonry structures, with regard to the response to seismic excitations. The types of masonry typologies which are considered are made of perforated clay units considered suitable construction systems for low-rise buildings (up to 3-4 storeys) in moderate seismic areas. Within the programme, tests were made at the EUCENTRE and at the University of Pavia laboratories on shear walls of different aspect ratios and different vertical loads, aiming to investigate the cyclic behaviour of walls affected by different failure mechanisms (flexure, shear or mixed) in dependence of a specific combination of parameters. The tests were used to obtain an experimental reference for the evaluation of strength, ductility, displacement capacity, energy dissipation, and they can be used also for the calibration of numerical models for nonlinear analyses with the same materials but different geometry, vertical loads and boundary conditions.

KEYWORDS: Experimental tests, in-plane cyclic response, masonry walls, clay units, failure mechanisms.

1. INTRODUCTION

This work has been carried out within the ESECMaSE Project, funded by the European Commission and aiming at improving the knowledge on the lateral in-plane response of masonry walls and the global seismic behaviour of entire buildings. The project is mainly focused on three typologies of blocks produced in Europe for new constructions: hollow clay, calcium silicate and lightweight aggregate concrete blocks.
Both numerical simulations and experimental tests have been carried out by the project partners. The activity of the University of Pavia has been mainly devoted to the in-plane cyclic testing of masonry piers. A completely new test setup has been designed, allowing different boundary conditions. A clear and repeatable procedure has been used for the whole testing campaign. A total of 28 large scale walls have been tested: in this paper only the results of ten perforated clay unit masonry walls are reported.

2. TEST SET-UP, INSTRUMENTATION AND TESTING PROCEDURE

The in-plane cyclic tests were carried out at the EUCENTRE Laboratory for Seismic Testing of Large Structures. The installation of the new test setup took advantage of the three-dimensional configuration of the strong floor and the L-shaped strong walls. The adopted test setup is shown in Figure 1(a). The walls were built on a 400 mm thick reinforced concrete footing, clamped to the strong floor by means of post-tensioned steel bars. A horizontal actuator applied a shear force to the top of the wall through a composite steel beam. The wall was restrained from out-of-plane deflections by a sliding restrainer system. Two vertical actuators applied the vertical load on the wall, reacting on a steel frame fixed on one of the strong walls of the laboratory. Figure 1(b) schematically shows the typical wall instrumentation with 25 displacement transducers installed on each wall.
The testing procedure considered two different boundary conditions: a “double fixed” system (rotation restrained at the top beam) and a “cantilever” system (free rotation at the top) with a constant vertical load applied at the top. The vertical force was initially gradually applied in order to estimate the compressive

Young's modulus of masonry. The horizontal load was applied with an initial force-controlled phase followed by a displacement-controlled loading history, performing three cycles for each target displacement level. Before the test, an estimate of the maximum shear strength was made, and a first repetition of three fully reversed cycles was performed by imposing, in a force-controlled way, a horizontal force equal to one fourth of the maximum estimated strength. Horizontal displacements were recorded. The procedure was then switched to a displacement-controlled one, in which the target displacements are multiple of the displacement measured in the first force-controlled phase, repeating three cycles for each target displacement. This method aimed to get sufficient points describing the ascending branch of the force-displacement envelope curve. Once the specimen approached its maximum shear strength the further target displacements were then chosen from a predefined sequence of drift-based displacement levels. The duration of each cycle was kept constant incrementing the actuator displacement rate proportionally to the cycle target displacement, as also done in past experimental campaigns (Tomazevic et al., 1993). The tests were stopped in case of critical damage conditions or at a horizontal top displacement larger than 2.0% drift.

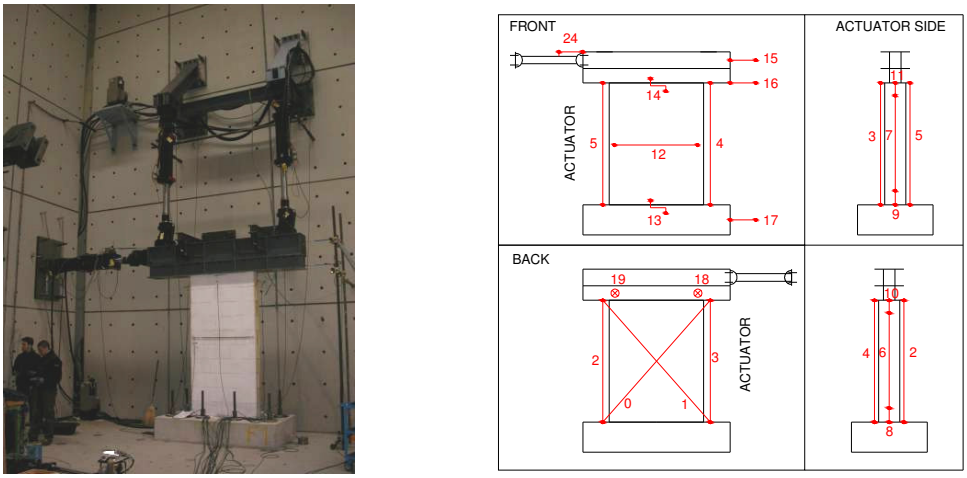

a) b)

Figure 1. Test set-up and instrumentation

3. TEST SPECIMENS AND MATERIAL PROPERTIES

Nine unreinforced and one confined perforated clay unit masonry walls were tested. Different kind of units and mortar were used. The dimensions and the details of the walls are summarized in Table 1, where l is the length, t is the thickness, h is the clear height and σ_v is the mean compression stress (N/l·t, with N the total vertical load) of the walls. In that table, the size of the clay units (length x thickness x height of the unit), the type of bedjoints and head joints, the boundary conditions of the cyclic tests and the vertical reinforcement are also reported. The levels of compression stress σ_v applied on walls CL04-CL10 correspond to the values of the most compressed walls in a typical Italian masonry construction. Lower values of vertical stress were applied on walls CL01-CL03 in order to reproduce the conditions of the same walls part of a large scale building tested in Ispra within the ESECMaSE project (Anthoine, 2007). The vertical holes of the clay units of walls CL01 and CL02 were completely filled with concrete. Wall CL02 was confined with one ϕ 16 mm diameter non-weldable steel bar placed at each end of the wall. In all the other walls the holes of the units were not filled. For walls CL01-CL03, thin layer mortar of class M10 (according to EN 998-2) was used; two different batches of pre-mixed general purpose (G.P.) mortar of class M5 were used for walls CL04-CL06 and for walls CL07-CL08 and finally, for walls CL09-CL10, thin layer pre-mixed mortar of class M10 was provided.
Several tests of characterization of the material properties were carried out at the laboratories of the University of Pavia and of the University of Munich (Magenes et al., 2008; Grabowski, 2005). In particular, tests on units, on mortar, on masonry wallets and on reinforcement steel were performed. The mean strength of the main tests carried out on the materials is reported in Table 1.

Table 1. Clay unit masonry piers.

Wall	l [m]	t [m]	h [m]	σ_v [MPa]	Unit size[mm]	Bed joints	Head joints	Bound. Cond.	Reinf.
CL01	1.50	0.175	2.5	0.31	373x175x249 Figure 2a)	Thin	Unfilled	Double fixed	NO, filled
CL02	1.50	0.175	2.5	0.33	373x175x249 Figure 2a)	Thin	Unfilled	Cantilever	1+1 ϕ 16, filled
CL03	1.00	0.365	2.5	0.14	247x365x249 Figure 2b)	Thin	Unfilled	Double fixed	NO
CL04	2.50	0.300	2.6	0.50-0.68	250x300x190 Figure 2c)	G.P.	Filled (G.P.)	Double fixed	NO
CL05	2.50	0.300	2.6	0.68	250x300x190 Figure 2c)	G.P.	Filled (G.P.)	Double fixed	NO
CL06	1.25	0.300	2.6	0.50	250x300x190 Figure 2c)	G.P.	Filled (G.P.)	Double fixed	NO
CL07	1.25	0.300	2.6	0.50	250x300x190 Figure 2d)	G.P.	Unf. (T+G)[1]	Double fixed	NO
CL08	2.50	0.300	2.6	0.68	250x300x190 Figure 2d)	G.P.	Unf. (T+G)	Double fixed	NO
CL09	1.25	0.300	2.6	0.50	250x300x230 Figure 2e)	Thin	Unf. (T+G)	Double fixed	NO
CL10	2.50	0.300	2.6	0.68	250x300x230 Figure 2e)	Thin	Unf. (T+G)	Double fixed	NO

[1] (T+G) stands for tongue and groove units (units with vertical mechanical interlocking).

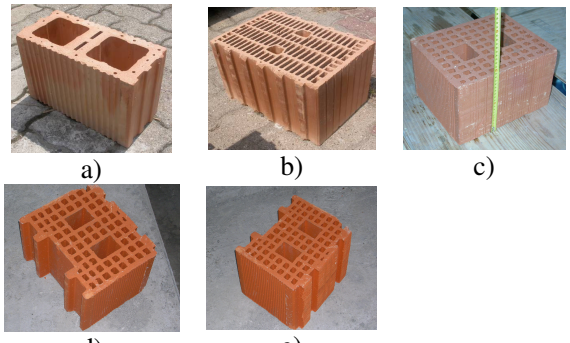

a) b) c) d) e)

Figure 2 Types of perforated clay units

Table 2. Mean strengths of materials from tests

Vert. compr. strength of unit b)	13.1 MPa
Vert. compr. strength of unit c)	15.1 MPa
Compr. strength of mortar for walls CL04-CL06	7.38 MPa
Compr. strength of mortar for walls CL07-CL08	10.6 MPa
Compr. strength of mortar for walls CL09-CL10	10.3 MPa
Vert. compr. strength of masonry for walls CL04-CL06	9.50 MPa
Vert. compr. strength of masonry for walls CL07-CL08	6.60 MPa
Vert. compr. strength of masonry for walls CL09-CL10	5.30 MPa
Shear strength for walls CL04-CL06 (from diagonal compression tests)	0.278 MPa
Yield strength of vertical reinforcement	476 MPa

4. EXPERIMENTAL RESULTS

Ductility, displacement capacity and energy dissipation issues are here discussed with reference to the specific experimental failure mechanisms. The results of the cyclic tests on the ten clay masonry piers in terms of hysteretic force-displacement curves are presented in Figure 3 (the top displacement δ measured at the lowest edge of the steel beam is considered).

4.1. Failure modes of the piers

The unreinforced wall CL01 was tested as a double fixed system. No diagonal cracks occurred during the test and the wall displayed a typical rocking behaviour without any significant strength degradation or relevant energy dissipation. With a top displacement larger than 50 mm (corresponding to a drift of 2.0%) a wide horizontal crack was clearly visible in the top and bottom corners of the panels due to tension stresses. The test was interrupted when the top displacement attained about 70 mm due to the stroke limits of the transducers; at that stage the wall was substantially undamaged (except for the horizontal cracks).

The wall CL02 was confined with 1 ϕ 16 bar at each end. The wall was tested as cantilever system. This wall has some similarity with a concrete wall with concentrated vertical bars at the ends since the large holes of the clay units were completely filled by concrete. No diagonal cracks occurred during the test. Energy dissipation was due to the yielding of the rebars. At a top displacement larger than 10 mm two vertical parallel cracks at the edges of the walls close to the position of the bars occurred, isolating two r.c. columns at the ends of the wall. Strength degradation after the attainment of peak strength was accompanied also by damage at the compressed corner. The test was interrupted when the top displacement attained more than 70 mm for reasons due to the stroke limits of the transducers and also for quite appreciable strength degradation.

The unreinforced masonry wall CL03 was tested with double fixed boundary condition. The level of the vertical stress was very low (0.14 MPa). No diagonal cracks in the units occurred during the test and the wall displayed a rocking behaviour without any significant strength degradation or relevant energy dissipation. With a drift

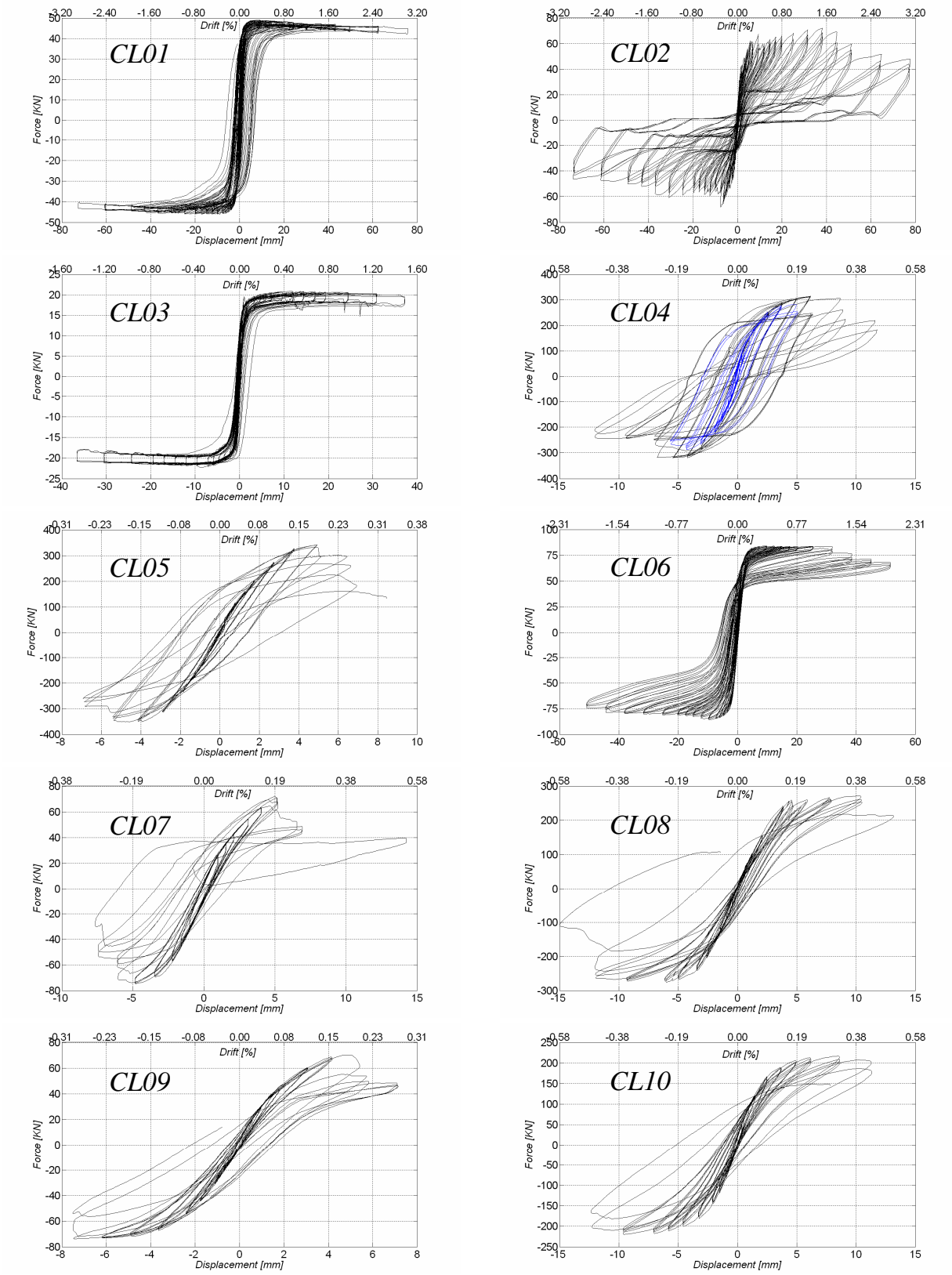

Figure 3 Experimental force-displacement curves

larger than 1.0%, horizontal and vertical cracks in the joints concurred to form a system of stepped diagonal cracks along the wall; these cracks closed during unloading without any loss of strength or stiffness. Moreover, wide horizontal cracks were clearly visible in the top corners of the panel due to tension stresses. At the bottom of the wall, a horizontal crack due to tension stresses formed at the bedjoints between the first and the second course of the masonry units. The test was interrupted when the top displacement attained about 37 mm for the large damage in the wall.

The vertical stress applied on the wall CL04 was initially equal to 0.50 MPa. Nevertheless, significant sliding along the joint between the steel beam at the top and the wall itself was shown after 7 cycles. It was then decided to increment the vertical stress up to 0.68 MPa. At this higher level of compression the wall developed a diagonal cracking failure. Still, the displacement measured at the top beam was found to have a significant component due to sliding. For this reason the hysteresis loops show a large dissipation that was not only associated to cracking in the panel but to a large extent by sliding.

Wall CL05 failed with diagonal shear cracks in the masonry units from corner to corner of the wall, at rather small top displacement (just beyond 0.25% drift). Spalling of some units also occurred. Large strength and stiffness degradation occurred after diagonal cracking. Before attaining this displacement level no evident damage was present except for small diagonal cracks in the units.

In the wall CL06 no diagonal cracks occurred during the test and the wall displayed a typical rocking behaviour with low energy dissipation. Strength degradation after the peak occurred since the resultant of the compression moved towards the centre of the panel for the concentration of the damage in the compressed corners. A wide horizontal crack was clearly visible in the top corners of the panel due to tension stresses. The test was interrupted when the top displacement attained about 50 mm (slightly less than 2% drift) after conspicuous strength degradation although displacement capacity reserves were probably still present.

Wall CL07 was constructed with T+G clay units and general purpose mortar. The wall failed with two diagonal shear cracks in the masonry units from corner to corner of the wall, at a rather small top displacement (just below 0.2% drift). Spalling of some units at the centre of the panel also occurred. Large strength and stiffness degradation occurred after diagonal cracking. Before attaining this displacement level no evident damage was present, therefore this wall displayed a rather brittle behaviour.

Wall CL08 was of the same typology of wall CL07 but with a length of 2.5 m. The wall failed by shear cracking with the occurrence of two diagonal cracks in the masonry units from corner to corner of the wall. This damage started to appear at a drift of 0.2-0.25% and the cracks developed in the panel up to a drift of 0.4 % when strength degradation occurred. Spalling of some units at the centre of the panel was also evident. The test was stopped for diffused damage and large strength degradation.

Wall CL09 had the same characteristics of wall CL07 but the bedjoints were made up with thin layer mortar instead of general purpose mortar. The failure mode of this wall was very similar to failure of wall CL07 both for the cracking pattern and for the maximum displacement capacity. The wall failed with two diagonal shear cracks in the masonry units from corner to corner of the wall, at rather small top displacement (below 0.25% drift). Strength degradation occurred after diagonal cracking.

Wall CL10 and wall CL08 showed similar failure modes since the two specimens had the same characteristics in terms of dimensions, vertical load applied and boundary condition. The only difference as respect to wall CL08 was the thin layer bedjoint. Diagonal cracks in the units started to be visible at a drift of about 0.20%. The wall failed with two diagonal shear cracks in the masonry units from corner to corner of the wall, at small top displacement corresponding to about 0.45% drift. The wall collapsed when strength degradation occurred after the corner to corner diagonal cracking.

4.2. Ductility and deformation capacity

A common approach to interpret the in-plane response of masonry walls is to idealize the cyclic envelope of the hysteresis loop with a bilinear envelope. In Figure 4 a possible definition of the parameters of the bilinear curve is given. The elastic stiffness k_{el} is obtained by drawing the secant to the experimental envelope at $0.70V_{max}$, where V_{max} is the maximum shear of the envelope. The ultimate displacement δ_u can be evaluated as the displacement corresponding to strength degradation equal to 20% of V_{max}. The value of the shear V_u corresponding to the horizontal branch of the bilinear curve can be found by ensuring that the areas below the cyclic envelope curve and below the equivalent bilinear curve are equal. Knowing the elastic stiffness k_{el} and the value of V_u it is possible to evaluate the elastic displacement δ_e as V_u/k_{el}. The ultimate ductility is defined as

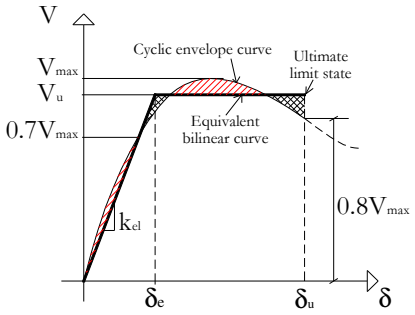

Figure 4. Hysteresis envelope and its bilinear idealization (Magenes and Morandi, 2008).

Table 3. Elastic stiffness, ultimate ductility, ultimate displacement and failure mechanisms.

Test	k_{el}^+ [KN/mm]	k_{el}^- [KN/mm]	δ_e^+ [mm]	δ_e^- [mm]	δ_u^+ [mm]	δ_u^- [mm]	μ_u^+	μ_u^-	$\mu_{u,min}$	(δ_u^+/h)	(δ_u^-/h)	$(\delta_u/h)_{min}$	Fail. Mech.
CL01[1]	59	38	0.8	1.2	75.9	72.6	95.7	60.6	60.6	0.0304	0.0290	0.0290	FLEXURE
CL02[3]	16	22	3.9	2.6	51.9	35.5	13.3	13.8	13.3	0.0208	0.0142	0.0142	FLEXURE
CL03[1]	27	35	0.8	0.6	37.2	36.6	48.5	59.6	48.5	0.0149	0.0146	0.0146	FLEXURE
*CL04[3]	115	115	2.5	2.6	9.1	9.4	3.7	3.7	3.7	0.0035	0.0036	0.0035	SHEAR
CL05[1]	106	123	3.2	2.8	6.5	6.8	2.0	2.5	2.0	0.0025	0.0026	0.0025	SHEAR
CL06[1]	40	40	2.0	2.0	51.5	50.8	25.9	25.3	25.3	0.0198	0.0195	0.0195	FLEXURE
CL07[3]	19	26	3.9	3.3	5.9	6.5	1.5	2.0	1.5	0.0023	0.0025	0.0023	SHEAR
CL08[1]	68	80	3.8	3.4	13.1	12.8	3.4	3.8	3.4	0.0050	0.0049	0.0049	SHEAR
CL09[3]	24	23	2.7	3.1	5.4	7.2	2.0	2.3	2.0	0.0021	0.0028	0.0021	SHEAR
CL10[1]	71	66	3.0	3.3	11.3	12.3	3.8	3.8	3.8	0.0043	0.0047	0.0043	SHEAR

Note 1: the superscripts $^+$ and $^-$ refer to the positive and negative shear-displacement envelope; h is the height of the piers. The superscript ^{i} after the name of the wall means that the reported results in terms of ultimate displacement are relevant to the i-th cycle (for example CL01[1] means that the ultimate displacement was attained during the first of the three cycles programmed for a given target displacement).

Note 2: the values associated to wall CL04 (denoted with *CL04) should be considered taking into account the way in which the wall was tested (test carried out in two phases with two different levels of axial force).

$\mu_u=\delta_u/\delta_e$. Ductility and displacement capacity were calculated for each wall considering the first, the second and third cycle envelope both for the positive and for the negative shear displacement envelope. To ease the discussion of the results, in Table 3, for the different masonry typologies, selected values of the elastic stiffness k_{el}, the elastic displacement δ_e, the ultimate displacement δ_u, the ultimate ductility μ_u, the ultimate drift δ_u/h and the failure mechanism are reported. The values in this table were taken from the envelope (first cycle, second cycle or third cycle) which has been considered as more representative of the results of the test on the specific wall with regard to ultimate displacement capacity.

Very high values of ductility and drift capacity were found for walls CL01 and CL03. This behaviour is typical of rocking-flexure failure. The maximum displacement attained for such walls was more related to the experimental set-up displacement capacity or to the local damage more than significant shear strength degradation. The confined wall CL02, tested as a cantilever, failed by flexure. High values of ductility were found although the maximum displacement was associated to significant shear strength degradation due to the damage at the compressed corner. In the wall CL06 no diagonal cracks occurred during the test and the wall displayed a typical rocking behaviour without any relevant energy dissipation. Strength degradation after the peak occurred since the resultant of the compression moved towards the centre of the panel for the concentration of the damage in the compressed corners. However, very high values of ductility and displacement capacity (a maximum drift of about 2%) were found.

Small values of ductility and ultimate displacement were instead found for the walls failing in shear. The maximum drift for the walls failing in shear did not exceed 0.5%, in some cases barely attaining 0.2%. The 2.5 m long wall constructed with general purpose mortar bedjoints and head joints (CL05) attained a very small value of ductility and deformation capacity. Walls CL08 and CL10, constructed with T+G units with unfilled head joints, having the same dimensions and the same vertical loads of wall CL05, were less resistant but attained a higher displacement capacity, approaching 0.4% drift. No evident differences in terms of ductility and in terms of displacement capacity were found for the walls with T+G units between different types of mortar

bedjoints. The slender wall CL07 with general purpose mortar bedjoints and the slender wall CL09 with thin layer mortar bedjoints showed very similar values of ultimate ductility (1.5 and 2) and of ultimate drift (0.23% and 0.21%). Same conclusions can be drawn for walls CL08 and CL10. In fact, the ultimate ductility and the ultimate drift for wall CL08 were 3.4 and 0.49%, whereas for wall CL10 were 3.8 and 0.43% respectively.
Very similar values of elastic stiffness were also found for the walls with T+G units between the two different types of mortar bedjoints.

4.3. Energy dissipation capacity

The dissipated hysteretic energy was examined in terms of equivalent viscous damping, which, given a single load–displacement cycle can be expressed as a function of the dissipated energy W_d and the elastic energy at peak displacement W_e: $\xi_{eq}=W_d/2\pi(W_e^{+}+W_e^{-})$. In Figure 5 the results of the calculated equivalent viscous damping ξ_{eq} are plotted as a function of the displacement ductility (δ/δ_e) of each cycle and considering the first, the second and the third cycle at each target displacement.

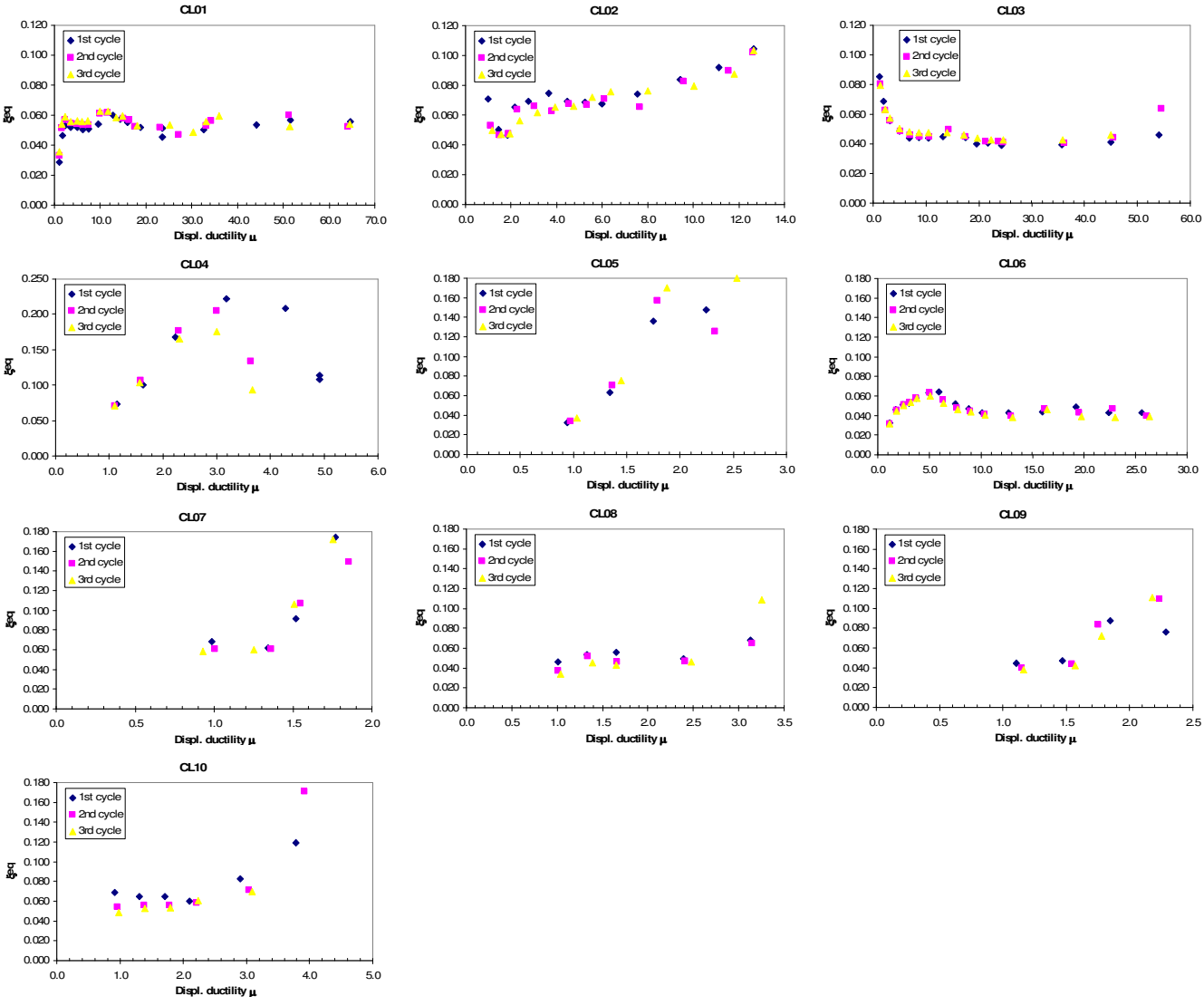

Figure 5 Equivalent viscous damping ratio calculated from the hysteresis loop as a function of displacement ductility ($\mu=\delta/\delta_e$)

The cycles of the walls CL01, CL02, CL03 and CL06 have low dissipation. All these walls failed in flexure. The equivalent viscous damping ξ_{eq} for unreinforced walls CL01, CL03 and CL06 was found to be around 5% and almost constant for all cycles. In the confined wall CL02 higher dissipation occurred because of the yielding of the vertical bars; the equivalent viscous damping increased linearly as a function of the ductility from 5 to 10%. The hysteresis loops of wall CL04 show large values of equivalent viscous damping that were not only associated to cracking in the panel but to a large extent by sliding along the joint between the steel beam at the top and the wall itself. However, except for wall CL04, the trend of the equivalent viscous damping was similar for all the walls that failed in shear. The damping increased as the ductility increased from 5% up to values higher than 10%. A clear distinction between shear and flexural failure can be noticed looking at the ξ_{eq}-μ plots.

5. CONCLUSIONS AND FUTURE DEVELOPMENTS

The results of a part of an experimental campaign on in-plane cyclic behaviour of perforated clay unit walls have been presented and discussed in terms of reference parameters for seismic design.
A wide variation in ductility and drift capacity has been reported depending on the failure mode which is in turn influenced by masonry typology, geometry, level of axial load and boundary conditions. When diagonal cracking in units is avoided, high drift capacities can be attained, sometimes exceeding 1.0% or more, whereas very brittle behaviour is reported when diagonal cracks develop through the units. In particular, very low drift capacity (below 0.25%) was reported in presence of high mean vertical compression stress (0.68 MPa). It appears therefore as an important seismic design criterion to limit compression stresses in walls to avoid bad performance, since the increase in shear strength due to axial compression may not compensate the dramatic reduction in deformation capacity.
No evident differences in terms of elastic stiffness, ductility, displacement capacity and shear strength were found for the clay masonry walls with T+G units between different types of mortar bedjoints. The walls with general purpose mortar bedjoints and the same walls with thin layer mortar bedjoints showed very similar values of ultimate ductility and of ultimate drift.
Further work will be dedicated to the interpretation of the results in terms of measured strengths, particularly important for the walls that displayed shear failure.

REFERENCES

Anthoine, A. (2007). D 8.1 Definition and design of the test specimen. *Report of WP 8, ESECMaSE Project*.

CEN - EN 998-2 (2003). Specification for mortar for masonry - Masonry mortar.

Grabowski, S. (2005). D 5.5 Material properties for the tests in WP 7 and 8 and the verification of the design model of WP 4. *Report of WP 5, ESECMaSE Project*.

Magenes, G. and Calvi, G.M. (1997). In-plane seismic response of brick masonry walls. *Earthquake Engineering and Structural Dynamics* **Vol. 26**, 1091-1112.

Magenes G., Morandi P., Penna, A. (2008). Test results on the behaviour of masonry under static cyclic in plane lateral loads. *Scientific Report of the Department of Structural Mechanics, University of Pavia,* **Report RS-01/08.**

Magenes G., Morandi P. (2008). Proposals for the evaluation of the q-factor from cyclic test results on masonry walls. *Scientific Report of the Department of Structural Mechanics, University of Pavia.*

Tomaževič, M. Lutman, M., Petković, M. (1993). Seismic behaviour of masonry walls: experimental simulation. *Journal of Structural Engineering, ASCE* **122 (9)**, 1040-1047.